Line-of-Sight Discovery in 3D Using Highly Directional Transceivers

Mahmudur Khan, *Member, IEEE*, Suman Bhunia, Murat Yuksel, *Senior Member, IEEE*, and Lawrence C. Kane

Abstract—Directional Radio Frequency (RF) / Free-Space-Optical (FSO) transceivers have the potential to play a significant role in future generation wireless networks. They are advantageous in terms of improved spectrum utilization, higher data transfer rate, and lower probability of interception from unwanted sources. Despite these advantages, communications using directional transceivers require establishment and maintenance of line-of-sight (LOS). Thus, establishment of the communication link or neighbor discovery plays an important role in mobile ad hoc networks with RF/FSO directional transceivers. We consider two nodes (Unmanned Aerial Vehicles (UAVs) or quadcopters) hovering in 3D space, each with one directional transceiver mounted on a mechanically steerable spherical structure/head, with which they can scan 360 degrees in the horizontal plane and 360 degrees in the vertical plane. We propose a novel scheme that deals with the problem of automatic discovery and establishment of LOS alignment between these nodes. We performed extensive simulations to show the effectiveness of the proposed neighbor discovery method. We also developed a proof-of-concept prototype and conducted experiments with it. The results obtained from both simulations and experiments show that, using such mechanically steerable directional transceivers, it is possible to establish communication links to similar neighboring nodes within several seconds without using GPS support.

Index Terms—Directional, 3D, RF, FSO, neighbor discovery, ad hoc, VANET, MANET, prototype

1 Introduction

The application of high gain directional antennas has attracted strong interest from the wireless research community especially for mobile ad hoc networks in the recent years [2], [3], [4], [5]. Directional antennas not only provide higher gain for signal reception but also makes faster data transfer possible compared to the traditional omni-directional ones. Using directional antennas for signal reception reduces interference caused from unwanted directions. This directionality improves spatial reuse and also lowers the probability of interception or detection by sniffers. All these advantages of directional antennas are suitable for tactical ad hoc networks where multiple entities desire to transmit high bandwidth data streams simultaneously with a requirement of lower interference and reduced probability of being jammed or detected [6], [7], [8], [9]. The higher data rate required for communication links to transmit more information between UAVs triggered the idea of employing directional transceivers to meet the increasing demand [10]. Equipping UAVs with such high-speed directional transceivers can enable a large set of applications involving transfers of very large wireless data. There are many different applications of UAVs, like surveillance for a military mission (e.g., observation behind enemy lines) or a civil mission (e.g., monitoring of a traffic jam or a disaster area, or to broadcast critical data at sport events) which require many sensors. UAVs with several sensors generate a lot of data which has to be delivered to either another UAV or a ground station [11].

Although directional transceivers provide the aforementioned benefits, communications using these transceivers are limited by the strict requirement of LOS alignment. Due to the reduced field-of-view compared to the omni-directional case, the transceiver of a node must face directly towards the neighboring node and vice versa. Even if the two directional antennas are within the communication range of each other, they cannot establish a link if they are not facing each other. Thus, the first and foremost thing to do for establishing a directional RF/FSO communication link is neighbor discovery.

In this paper, we propose a novel method for neighbor discovery and establishing a communication link between two nodes hovering in 3D space (Fig. 1). We assume that each node is equipped with a highly directional FSO/RF transceiver mounted on a mechanically steerable spherical head. Thus, the transceivers can be steered for scanning 360 Degree in the horizontal plane and 360 Degree in the vertical plane. Further, we assume that there is no GPS available for exchanging location information. We show that using the mechanical steering capability to control the rotation of the transceivers, the problem of neighbor discovery or detection of LOS for link establishment can be dealt with effectively. Although, for smart RF transceivers/antennas with adaptive beamforming capability, mechanical steering may not be required. These antennas are useful in short distance communication where

- *M. Khan and M. Yuksel are with the Department of Electrical and Computer Engineering, University of Central Florida, Orlando, FL 32816. E-mail: mahmudurk@knights.ucf.edu, Murat.Yuksel@ucf.edu.*
- *S. Bhunia is with the Department of Computer Science and Engineering, University of California, Davis, CA 95616. E-mail: sbhunia@ucdavis.edu.*
- *L.C. Kane is with the Department of Computer Science, University of Central Florida, Orlando, FL 32816. E-mail: lawrenceckane@gmail.com.*

Manuscript received 20 Nov. 2017; revised 3 Oct. 2018; accepted 28 Nov. 2018. Date of publication 10 Dec. 2018; date of current version 31 Oct. 2019. (Corresponding author: Mahmudur Khan.)
For information on obtaining reprints of this article, please send e-mail to: reprints@ieee.org, and reference the Digital Object Identifier below.
Digital Object Identifier no. 10.1109/TMC.2018.2885061

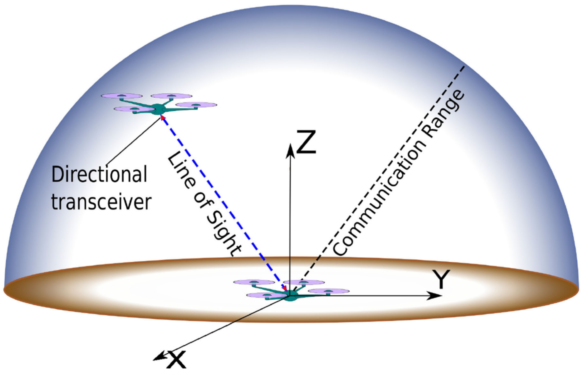

Fig. 1. Schema of UAVs with directional antennas.

range is not important but instantaneous switching between the beam directions is desired. However, adaptive beamforming antenna comes with their own limitations such as lower power, smaller accuracy in forming the desired beam pattern, and undesired sidelobes. Thus, in many applications, such as military flight communication where long distance communication is desired but the beams are not required to shift with higher agility, directional RF antennas with fixed beamwidth are used [12], [13]. These antennas are mechanically oriented towards the LOS. We also assume the availability of an omni-directional RF link (or a beacon from a base station), using which the nodes can synchronize the search for each other. Any RF frequency should work as the omni-directional channel that is suitable for UAV communication. Note that, higher frequencies such as 5 GHz ISM band incurs heavy path loss in long distance communication. 900 MHz ISM band is more suitable for this kind of operation since nodes can communicate over a few kilometers. Once synchronization is complete, the nodes operate in-band and only use the directional transceivers to discover each other.

The basic idea for our neighbor discovery approach is to rotate the transceivers of each node with a given angular speed. One node (Master) starts a three-way handshake by sending a Beacon message and the other node (Slave) waits for the Beacon message. Upon reception of the Beacon, the slave node stops rotating its transceiver and sends an acknowledgment (B-ACK). When the master receives the B-ACK, it also stops scanning and sends an ACK completing the handshake.

1.1 Contributions and Novelties

- A novel method for two nodes in a 3D environment to discover each other without any knowledge of the neighbor's location using only one highly directional transceiver each and an additional omni-directional link (or a base station periodically sending beacons) for initial synchronization.
- A modified helical path to scan the 3D space.
- A prototype to evaluate the performance of the proposed discovery method.
- Illustration through simulations and real test-bed experiments that the proposed technique helps complete neighbor discovery within acceptably small time period.

1.2 Key Insights

- We observed from the simulations that fully in-band neighbor discovery is possible within 0.36 seconds if the divergence angle of the transceiver is 20 Degree and the angular speed is 300 rpm (rotations per minute).
- We also observed from the simulations that the ideal value of the angular speed is $1.5 \times \omega_s$, where ω_s is the sufficient angular speed that ensures neighbor discovery within one complete scan of the surrounding 3D space.
- From the experiments, we observed that a quadcopter on the ground can discover another hovering quadcopter within 2.75 seconds when the angular speed of the transceivers are 180 Degree$/s$ and divergence angle of 24 Degree.
- We observed that, 33 nodes can all discover each other within 3.96 seconds with transceivers of divergence angle of 25 Degree and angular speed of 300 rpm.

The rest of the paper is organized as follows: In Section 2, we survey the relevant background on directional transmission and neighbor discovery. The proposed methodology, theoretical analysis and the algorithms are described in Section 3. In Section 4, we illustrate the simulation scenarios and discuss the results. We provide the details of the proof-of-concept prototype and analyze the experimental results in Section 5. Finally, we summarize and conclude the paper in Section 6.

2 Background

In this section, we first present the motivation for using directional transceivers in both FSO and RF communications. Then, we discuss the existing literature on neighbor discovery protocols for directional transmission.

2.1 Directional Wireless Communication

Directional wireless antennas/transeivers are desired by applications that require longer communication range, high spatial reuse and low probability of detection. The higher gain of directional transceivers helps achieve larger communication distance and faster data transfer speed compared to omni-directional transceivers. Recent reports demonstrate that upto 10 Gbps data transfer rate has been achieved using lasers and 20 Gbps data rate over 13 km using mmWave technology [14], [15]. Omni-directional antennas transmit in directions other than the intended ones, and thus, increase interference and reduce communication range. Nodes with omni-directional antennas use complex MAC protocols to avoid transmission collision and interference coming from other transmitters. Directional antennas provide spatial reuse that allows multiple transmitter-receiver pairs to communicate simultaneously without interfering with each other's communication [2], [16]. Also, the combination of higher gain and spatial reuse results in increased capacity [17], [18]. Moreover, as directional antennas transmit at or receive from specific directions, they not only reduce intereference but also enhance security by reducing the probability of interception and detection [4], [18], [19], [20], [21].

2.2 Directional Neighbor Discovery

Neighbor discovery for directional RF has been well explored. Choudhury et al. [16] have designed a MAC protocol for ad hoc networks with directional transmitter and omni-directional receivers. An et al. [22] proposed a handshake-based self-adaptive neighbor discovery protocol for ad hoc networks with directional antennas. They also consider directional transmitters and omni-directional receivers for neighbor discovery while frequency of operation is determined on the run. Ramanathan et al. [18] presented UDAAN, the first full system deployment of an ad hoc network utilizing directional antennas. It uses heartbeat messages to exchange the position information and uses GPS clock cycle synchronization for neighbor discovery. This prototype uses omni-directional antennas for establishing the connection with new neighbors. Vasudevan et al. [23] have proposed a neighbor discovery protocol for ad hoc networks with directional RF. They have considered that a node can either transmit or receive. The protocol uses an optimal value of probability for transmitting beacon message at random directions. They have also described a gossip-based neighbor discovery algorithm, where location information of an undiscovered neighbor is taken from GPS and from neighbors who have already discovered it.

Another design dimension has been the consideration of directionality for both transmitters and receivers. Jakllari et al. [24] presented a neighbor discovery method that uses both directional transmitters and receivers. It proposed a polling-based MAC protocol for MANETs where all nodes are synchronized in terms of the polling slots. It allocates slots for discovering new neighbors when all nodes point to random directions and advertise for neighbor discovery. It also provides a framework to compute neighbor discovery time.

One design direction has been to consider nodes with no clock synchronization but with highly directional transceivers. Chen et al. [25] and Wang et al. [26] presented two different neighbor discovery processes that use only a single directional transceiver without any clock synchronization. We proposed a similar in-band LOS discovery algorithm in [27], that requires no aid from GPS or any additional omni-directional channel. But, all these works consider nodes present in 2D wireless networks. Recently, in [28], we presented an in-band LOS discovery method for nodes deployed in a 3D ad hoc network that does not require any clock synchronization or a priori location information. However, due to the lack of coordination of nodes via an omni-directional channel, these schemes result in significantly larger discovery times than our work.

A promising design approach has been to utilize scanning over discretized time slots. Zhang et al. [3], [29] proposed two such algorithms for neighbor discovery with directional RF communication. The authors considered that the nodes are synchronized and use synchronized slots to transmit neighbor discovery requests. In a generic algorithm, each node transmits message with probability of 0.5 in random direction. In a scan-based algorithm, nodes use a predefined scan sequence of antenna direction. Steenstrup et al. [30] proposed a similar scan-based algorithm. These works provided excellent analysis on the number of slots and scans required to complete the neighbor discovery. The scan sequences are considered to be combinations of beams pointed at specified directions. Yet, they work in settings where synchronized time slots is realizable at each node. In our work, we consider continuous rotation of transceivers for scanning the surrounding 3D environment.

In this paper, we explore a hybrid approach where nodes are *synchronized* initially via an omni-directional channel (or a beacon from a base station) and then autonomously search for each other over a continuous timeline. We consider the availability of an omni-directional RF only for initializing the neighbor discovery process. A node is neither aware of its own position nor the neighbor's position. After the initialization, the RF link becomes inactive and the nodes use only the directional transceivers for discovering each other. We present a continuous scanning path covering a sphere in the form of a modified helix to be followed by the transceiver beams and the nodes are assumed to be situated in a 3D wireless network. Without any initial synchronization, the problem of neighbor discovery becomes harder and requires significantly longer discovery times. Such discovery schemes (e.g., [25], [26], [27] for 2D, and [28] for 3D networks) would be more useful in scenarios where clock synchronization or additonal communication channels are not available. For a fair comparison in terms of discovery time, we compared our technique to [3], which also allows initial synchronization and considers nodes in a 3D ad hoc network.

3 Theory

3.1 Assumptions for Propoosed Model

- *Mode:* The mode of communication between the nodes can be either half-duplex or full-duplex. We considered half-duplex communications for this work.
- *Nodes in 3D:* The nodes hover in 3D space and are within the communication range of each other.
- *Directional:* Both the transmitter and the receiver of a node are directional and face towards the same direction and rotate together. The receiver can receive signal from a neighbor that is within its main beam and the transmission beam of the neighbor must face towards it.
- *Transceiver rotation:* The nodes can rotate their transceivers 360 Degree in the horizontal plane and 360 Degree in the vertical plane using mechanically steerable heads.
- *Supplementary channel:* At the start of the discovery phase an additional omni-directional RF channel is used. The nodes are not equipped with any location tracking device such as GPS.

3.2 Transceiver Rotation in 3D space

As the distance between the transmitter and receiver of a node is very small compared to the communication range, we use one beam pattern to indicate both the transmission and field-of-view areas. Fig. 2 shows such a beam. We approximate the beam with a cone of height r and radius $r \tan \beta$, where r is the maximum communication range of the transceiver and β is the divergence angle (half angle from the axis of propagation) for transmissions. The angle of field-of-view is 2β for receptions. The orientation of the beam is denoted by r, θ, ϕ. In this paper, we shall use the Polar and Cartesian coordinates interchangeably and the corresponding conversion rules are given below.

$$\begin{cases} r = \sqrt{x^2 + y^2 + z^2} \\ \theta = \arccos(z/r) \\ \phi = \arctan(y/x) \end{cases} \Leftrightarrow \begin{cases} x = r \sin\theta \cos\phi \\ y = r \sin\theta \sin\phi \\ z = r \cos\theta. \end{cases} \quad (1)$$

3.3 Neighbor Discovery

As stated earlier, we consider two nodes hovering in 3D space. There are two main stages in the proposed neighbor discovery method: i) initialization and ii) 3D scanning. We briefly describe the two stages below (Fig. 3).

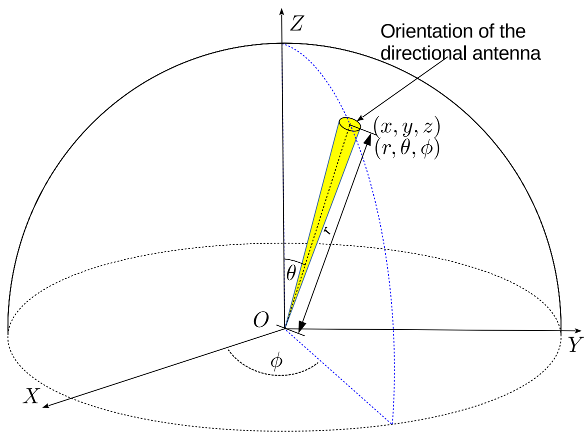

Fig. 2. Orientation of directional antenna in 3D sphere.

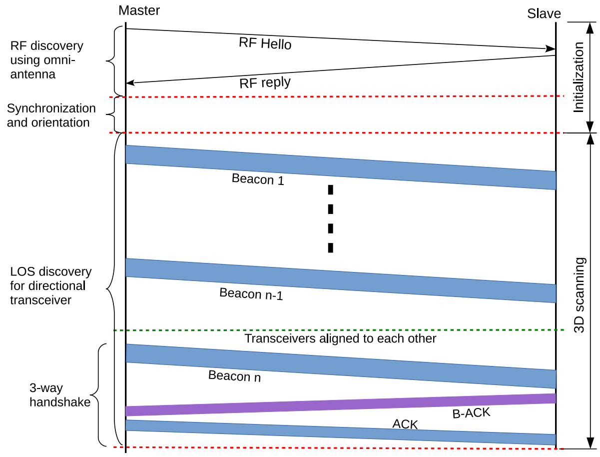

Fig. 3. Timing diagram of neighbor discovery.

3.3.1 Initialization

In the initialization stage, the nodes use their omni-directional transceivers to find the existence of a neighbor node through a common RF channel (very low data rate compared to directional transceivers). Since we consider the absence of GPS, the nodes do not know their location and hence cannot share their location information to each other. In this stage, one of the nodes agrees to act as master and the other one as slave. Assuming that each node has a unique ID, the one with the higher ID number can become the Master. Also, there are several leader election algorithms which can be used to select the Master node. Leader election algorithm is a widely researched topic in ad hoc netowrks, and a survey of such can be found at [31], [32], [33], [34], [35]. Our mechanism can be used with any of these proposed leader election algorithms. The master agrees to only transmit Beacon messages, and the slave acts as a receiver. The nodes decide to rotate their transceivers with same angular speed and direction on the horizontal plane.

3.3.2 3D Scanning

In this stage, the nodes use only their directional very high data rate RF/FSO transceivers for LOS discovery. The master sends a beacon through the omni-directional RF channel to the slave which kicks off the 3D scanning. The master node starts the 3D scanning with its transceiver facing in the upward direction. The slave node faces its transceiver downward at the start of 3D scanning. The master node rotates its transceiver following a modified spiral path (explained in Section 3.4) as shown in Fig. 4a. While rotating the transceiver, it sends a Beacon message periodically. The slave node also rotates its transceiver in a similar modified spiral path starting from the bottom end of the sphere. It waits for a Beacon message to arrive from the master node. Once a Beacon message is received, it stops rotating its transceiver and sends an acknowledgment message (B-ACK) to the master. Upon receiving the B-ACK message, the master also stops rotating its transceiver and does not send Beacon messages. It sends an ACK message to the slave completing the three-way handshake (Fig. 3). This completes the neighbor discovery and a communication link is established between the nodes.

3.4 Modified Helix Movement

To make the motor rotation smooth, we consider the transceiver beams to rotate in a spiral pattern and scanning in the 3D space for discovering the LOS between neighbor nodes. Fig. 4a illustrates a sample path taken by the beam. The dotted blue line denotes the path of the normal of the beam. We consider the range of the beam to be the radius of the sphere created by the modified spiral. We can simply imagine the idea of covering a tennis ball with a narrow tape. In that case, the width of the tape is same as the diameter of the transceiver beam. For better coverage, the distance between two lines in Fig. 4a should be equal for all the lines.

Fig. 4b provides a side view of the transceiver beam. Fig. 4c provides the 2D projection of the cross section of the beam in vertical (θ) and horizontal (ϕ) planes. Assume that at some time t, the normal of the beam is directed at point e. The path or trajectory of the normal is plotted in the picture. As the beam normal is rotating in a spiral, the path taken by the beam in the upper floor of the spiral is also plotted in the picture. As the beam moves from right to left (from h to g) in a continuous motion, a point within the square $abcd$ will be inside the circle with origin at e for a longer period of time, compared to a point lying outside the square $abcd$ but within the circle with origin at e. Thus, the width of the coverage of the beam movement (γ) can be calculated as follows:

$$2\gamma^2 = (2\beta)^2 \quad \Rightarrow \gamma = \sqrt{2}\beta. \tag{2}$$

As we have determined the width of the coverage, the number of rotations of the spiral (n) can be determined as:

$$n = \frac{\pi}{\gamma} = \frac{\pi}{\sqrt{2}\beta}. \tag{3}$$

With n rotations, the whole 3D space will be scanned and if there is a neighbor within the communication range, it could be discovered during this 3D scan.

3.4.1 Rotational Speed

We have found the trajectory to be followed by the transceiver beam to scan the whole 3D space. Now, we need to consider the angular speed of the transceiver so as to maximize the probability of neighbor discovery during the 3D scan. The maximum angular speed will be limited by the time required to complete 3-way handshake. Let us consider that the total time required to send Beacon, receive B-ACK and then to send ACK is τ. Incorporating transmission delay (t_{tran}), propagation delay (t_{prop}) and processing delay (t_{proc}) at both ends. τ can be calculated as:

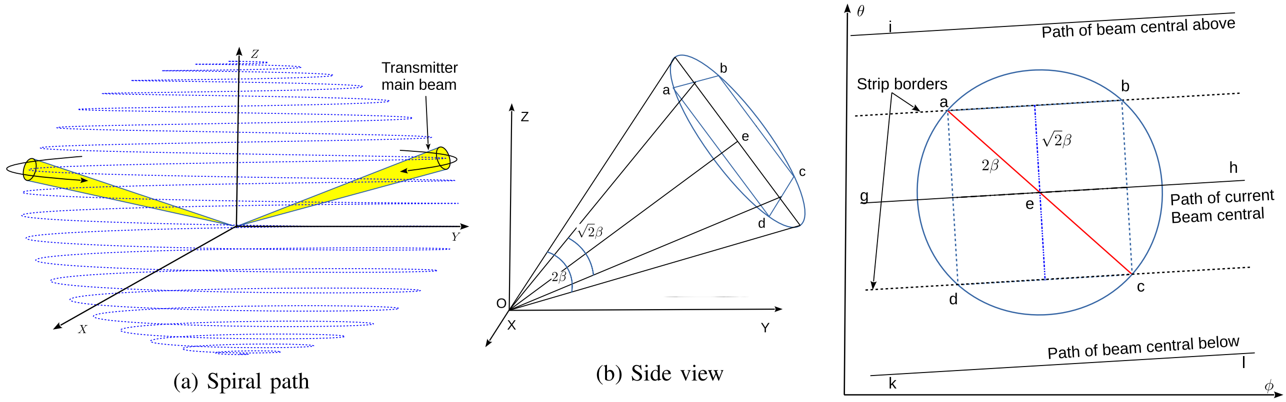

(a) Spiral path (b) Side view (c) Beam Cross Section

Fig. 4. Depiction of beam scan trajectory.

$$t_{tran} = \frac{\text{Beacon size} + \text{B-ACK size} + \text{ACK size}}{\text{data rate}} \tag{4}$$
$$\tau = t_{tran} + 3 \times t_{prop} + 2 \times t_{proc}.$$

t_{prop} will vary with distance between the nodes but we can consider a maximum propagation delay as the time required for the signal to propagate within transmission range which is in the order of nano seconds. t_{proc} can also vary depending on the hardware and processor workload at that moment.

From Fig. 4c, we can establish a relationship between the maximum angular speed the 3-way handshake time. If the neighbor node lies anywhere inside the $abcd$ square, the nodes will have $\frac{\gamma}{\omega}$ time to face each other. But, when they start facing each other the master may not start transmitting Beacon immediately, rather since the master may still have been transmitting the last Beacon. So, to assure that the nodes discover each other successfully, the time they face each other must be greater than 2τ. Although the necessary condition for discovery is $\gamma/\omega \geq \tau$, the sufficient condition will be:

$$\frac{\gamma}{\omega} \geq 2\tau \Rightarrow \omega \leq \frac{\beta}{\sqrt{2}\tau}. \tag{5}$$

Since the nodes synchronize themselves at the beginning and rotate the transceivers with same angular speed ω, they will be able to discover themselves as long as (5) holds true.

3.4.2 Suitable Modified Helix Equation

We have discussed the working principle of the beam scanning and the transceiver rotation in 3D space. Now we need to determine the path for the beam and its corresponding equations. We start with the equation of helix as provided in (6) below. A variable s is varied from -1 to 1 and the position is calculated in Cartesian coordinates (x, y, z). Fig. 5 plots the 3D view and the 2D projection of the path with this equation.

$$\begin{cases} s & \in [-1, 1] \\ \rho & = 1 \\ x & = \rho \sin(sn\pi) \\ y & = \rho \cos(sn\pi) \\ z & = sn\pi. \end{cases} \tag{6}$$

Note that for regular helix, the diameter of the spiral stays the same on the horizontal plane. So, we modified the equation of the helix and varied the diameter as a *cosine* function of s. In this case, the diameter of the spiral is 1 at the equator and 0 at the two poles. We also varied the movement along the z axis as a *sine* function of s. The equations of the modified helix are given in (7) and Fig. 6 illustrates the trajectory in 3D and 2D projections.

$$\begin{cases} s & \in [-1, 1] \\ \rho & = \cos(s\pi/2) \\ x & = \rho \sin(sn\pi) \\ y & = \rho \cos(sn\pi) \\ z & = \sin(s\pi/2). \end{cases} \tag{7}$$

Now, replacing x, y and z from (7), we can see that, $\sqrt{x^2 + y^2 + z^2} = 1$. So, the distance of a particle following this trajectory, from the center is the same for all values of s. If we vary s from -1 to 1, the beam scans the whole sphere. Thus, (7) represents the desired modified helix.

Theorem 1. *If two nodes are within the communication range r, initially orient their transceiver in opposite directions and rotate with same angular speed then they will be able to discover each other within one complete scan of their respective surrounding spherical volume with radius r as long as $\omega \leq \frac{\beta}{\sqrt{2}\tau}$, where ω is the angular speed, β is the divergence angle and τ is the three-way handshake time.*

Proof. We prove this by contradiction. Let us assume that two nodes A (master) and B (slave) are within the communication range of each other and follow the proposed neighbor discovery method. Then there are only 3 possible scenarios which can result in the nodes not discovering each other:

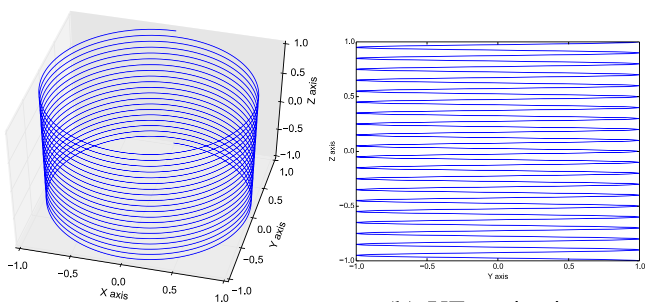

(a) 3D view (b) YZ projection

Fig. 5. Regular helix using (6).

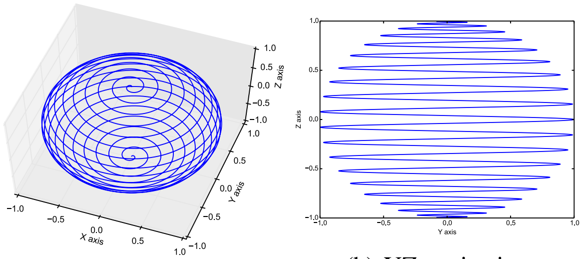

(a) 3D view (b) YZ projection

Fig. 6. Modified helix using (7).

- (i) B is not covered by A's transmitting beam.
- (ii) B is covered by A's transmitting beam but they do not have enough time to complete the three-way handshake.
- (iii) When A's transceiver is pointing towards B, B's transceiver is not pointing towards A.

Let us first look at Fig. 4c. The path of the beam's normal follows the gh line. The θ and ϕ coordinates have a range between $[-\pi, \pi]$. For a point to be not covered by the transmitting beam, it must be located at a point further than β from the line gh (i.e., outside the circle centered at e). Now, we know that, the distance between two paths like ab and cd is π/n, which (from (3)) is less than 2β. As the distance between two such lines is less than 2β, a point cannot be at a distance more than β from line gh. Thus, (i) is not possible.

Now, a node within the area $abcd$ will have at least $\frac{\beta}{\sqrt{2}\omega}$ amount of time for completing the three-way handshake. From (5), we know that the nodes will have at least τ amount of time for completing the discovery. Thus, (ii) is also not possible.

If (i) and (ii) are not possible, then the only possibility for the nodes to not discover each other is if they were not pointing towards with each other. Now, nodes A and B synchronize with each other in the *initialization* phase, and, they scan their transceivers at the same speed and direction (clockwise/counter-clockwise), starting from opposite transceiver orientations, i.e., one facing upward ($\theta = 0, \phi = 0$) and the other downward ($\theta = \pi, \phi = \pi$). So, when A faces at any direction (θ', ϕ'), B will face at $(\theta' + \pi, \phi' + \pi)$. If B is located at (θ'', ϕ'') with reference to A, when A points its transceiver at (θ'', ϕ''), B points its transceiver at $(\theta'' + \pi, \phi'' + \pi)$. So, both nodes point their respective transceivers towards each other at the same time. Thus, (iii) is not possible as well. □

3.5 Average Neighbor Discovery Time

Let us consider a scenario where the master node is located at position $(0, 0, 0)$, and the slave node at position $(0, 0, z_i)$. Let us consider the best case where the master starts scanning its beam from $\phi = 0, \theta = 0$, and the slave begins scanning from $\phi = 0, \theta = \pi$. In this case, the nodes will immediately find each other and the discovery time will be $\approx \tau$, which is the time to complete the 3-way handshake. Now, consider the worst case where the master starts scanning its beam from $\phi = 0, \theta = \pi$ and the slave begins scanning from $\phi = 0, \theta = 0$. In this case, the neighbor discovery time will be T_{scan}, which represents the time required to complete a full scan of the surrounding 3D environment. We can write T_{scan} as follows:

$$T_{scan} = \frac{1}{\omega}\int_{-\pi}^{\pi} \tan^{-1} \frac{\sqrt{\left(\frac{\partial x}{\partial s}\right)^2 + \left(\frac{\partial y}{\partial s}\right)^2 + \left(\frac{\partial z}{\partial s}\right)^2}}{\sqrt{x^2 + y^2 + z^2}} ds$$
$$= \frac{1}{\omega}\int_{-\pi}^{\pi} \tan^{-1} \sqrt{(\frac{\partial x}{\partial s})^2 + (\frac{\partial y}{\partial s})^2 + (\frac{\partial z}{\partial s})^2} ds. \quad (8)$$

Here, ω is the rotational speed of the transceivers. So, assuming the nodes are placed randomly the average neighbor discovery time is:

$$t_{avg} = \frac{\tau + T_{scan}}{2}. \quad (9)$$

Combining (7), (8), and (9), we can obtain t_{avg}. Note that (9) assumes the nodes are randomly placed with respect to each other. In practice, the nodes will likely be placed in a more correlated manner. In particular, the nodes will likely be spatially correlated over the vertical plane, e.g., they will be flying relatively at similar heights. However, picking the unfavorable case, we assume that the nodes are uniformly distributed across both horizontal and vertical planes in this work.

3.6 Multiple Neighbor Discovery (MND)

The proposed neighbor discovery algorithm can be applied to discover multiple neighbors, i.e., more than two nodes in the network. We propose two different approaches:

3.6.1 *Iterative MND (I-MND)*

Let us consider that there are M nodes in an ad-hoc network. So, each node has to discover $M-1$ neighbors. In the *initialization* phase, each node uses the available omnidirectional RF channel to inform the neighbor nodes in the network about its presence. So, each node is aware of the number of nodes in the network. The nodes then use a leader election algorithm [31], [32], [33], [34], [35] to elect one of the nodes as the master. The remaining $M-1$ nodes are considered as slaves. The master operates in transmission mode and the slaves operate in receive mode. Then, the nodes progress to the 3D scanning stage as described in Section 3.3.2. Since, only the master is in transmission mode, there is no possibility of packet collision. Thus, the master can discover $M-1$ slaves within one complete scan of the surrounding 3D network. A slave stops scanning as soon as it discovers the master and returns to the *initialization* phase. The master returns to the *initialization* phase after discovering all $M-1$ neighbors. Now, the $M-1$ slaves execute the leader election algorithm to elect a new master and perform 3D scanning in the same manner. This time, the 3D scanning ends when the master discovers $M-2$ neighbors. This procedure is continued until each node discovers its $M-1$ neighbors. Assuming the time to discover $M-1$ slaves by the first elected master as t_{M-1}, the time to discover $M-2$ slaves by the second elected master as t_{M-2}, and so on, the total neighbor discovery time using the I-MND approach is: $T_{I-MND} = \sum_{n=1}^{M-1} t_n$

3.6.2 *Logarithmic MND (L-MND)*

Here, we propose another approach for discovering multiple neighbors by modifying a deterministic scan-based algorithm *SBA-D* [3]. In *SBA-D*, if there are M nodes in the network, each node is assigned a unique identifier of $\log_2\lceil M\rceil$ bits. For example, if there are 8 nodes, they are

TABLE 1
Simulation Parameters

Symbol	Meaning	Value
P_t	Transmitter source power	-43 dBm
ξ	Transmitter radius	0.3 cm
ζ	Receiver radius	3.75 cm
σ	Attenuation coefficient	0.0508*

**For visibility of 20 km and wavelength of 1,550 nm [37].*

assigned the identifiers from 000 to 111. We assume that the nodes use the omnidirectional RF channel to elect a master as described in Section 3.6.1 and the master assigns the identifiers to all the nodes. The nodes then start 3D scanning at the same time and perform a full scan. In the jth scan, if the jth digit of a node's identifier is 1, it operates in reception mode and if it is 0, it operates in transmission mode. It was shown in [3] that, using this scheme, each node can discover all its neighbors within $\log_2\lceil M\rceil$ scans of the 3D network without taking the effect of collision into account. But, in this scheme, a node can receive packets from multiple neighbors at the same time. So, collision of packets might occur during the neighbor discovery process. So, in the L-MND aprroach, we consider the effect of collision. A node may not be able to discover all its neighbors within $\log_2\lceil M\rceil$ scans if collision occurs. Let us assume that, $M' \leq M$ nodes missed at least one node during $\log_2\lceil M\rceil$ scans because of collision. These M' nodes will again be assigned new identifiers of $\log_2\lceil M'\rceil$ bits and the *SBA-D* scheme will be performed. This procedure is continued until each node discovers all its neighbors.

4 Simulations and Results

We performed MATLAB simulations to analyze the effectiveness of the proposed directional neighbor discovery method. We considered DJI Matrice 100 (M100) drones [36] as the nodes. We considered a simulation region of $R_{max}/\sqrt{3} \times R_{max}/\sqrt{3} \times R_{max}/\sqrt{3}$, so that the nodes are within each other's maximum communication range R_{max}. We considered master node's hovering position as the origin. We repeated the simulations 2,000 times and randomly chose the hovering position of the slave node with different seeds for each simulation run. We assumed (R_{max}) of $25\mathrm{m}$, $50\mathrm{m}$, $75\mathrm{m}$ and $100\mathrm{m}$. We considered the divergence angles of the transmitters as β (half angle from the axis of propagation) and field-of-view (FOV) of the receivers to be 2β, where β had values of 3, 5, 10, 15, 20 and 25 Degree. We considered rotational speeds of $30 - 300$ rpm (rpm stands for rotations per minute and $1\ \mathrm{rpm} = 6^\circ/\mathrm{s}$) for the transceivers.

We assumed the nodes to be equipped with free-space-optical (FSO) transceivers (LEDs as transmitters and photodiodes as receivers). The received power and the maximum communication range of an FSO transceiver is affected by Lambertian loss, atmospheric attenuation and geometric attenuation. We calculated the received power P_{rcv} of a node's transceiver from the following relations [37]:

$$P_{rcv} = \cos\delta \times \Big(P_t - 10\log_{10} e^{-\sigma R\cos\delta} - 20\log_{10}\frac{\zeta}{\xi + 200\beta R\cos\delta}\Big), \tag{10}$$

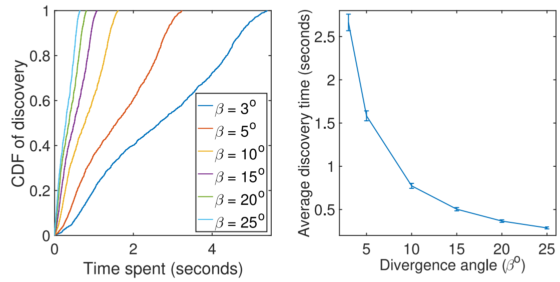

Fig. 7. CDF and average discovery time (95 percent confidence interval) for $\omega = 300$ rpm.

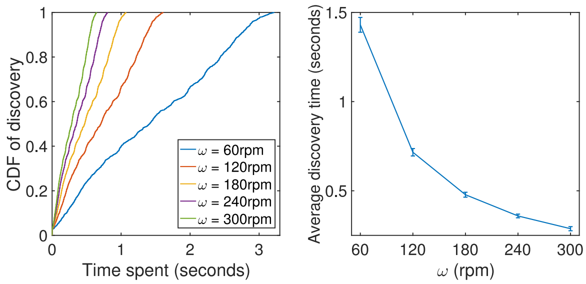

Fig. 8. Effect of ω on neighbor discovery time for $\beta = 25^o$ (95 percent confidence interval).

where R is the distance between the nodes in meters, δ is the radial distance of a node from its neighbor's beam's axis of propagation, P_t is the transmitter's source power in dBm, S is the receiver's sensitivity in dBm, ξ is the transmitter radius in cm, ζ is the receiver radius in cm, β is the divergence angle of transmitter in mRad, and σ is is the attenuation coefficient consisting of atmospheric absorption and scattering (Table 1).

4.1 Single Neighbor

In this section, we consider the case when there are only two nodes in the network. We performed simulations to observe how the proposed neighbor discovery method performs as the divergence angle is increased. We also want to observe how changing the angular speed of the transceiver affects the average neighbor discovery time.

Fig. 7 shows the cumulative probability (CDF) and the average neighbor discovery time for transceivers with different divergence angles β, for angular speed $\omega = 300$ rpm and $R_{max} = 100$ m. We can observe that the discovery time reduces more than linearly as the divergence angle increases. For example, the average discovery time is 2.66 s for $\beta = 3^\circ$, but it is only 0.28 s for $\beta = 25^\circ$. As presented earlier in (8) and (9), the neighbor discovery time is directly proportional to the time taken to scan the surrounding 3D space. This scannig time depends on the number of rotations n of the spiral or modified helix. From (3), we see that $n \propto 1/\beta$. Thus, the average neighbor discovery time $t_{avg} \propto 1/\beta$, and this can be observed in Fig. 7. Moreover, larger values of divergence angle or field-of-view (FOV) provides larger coverage volume, and thus, results in smaller discovery times.

In Fig. 8, we show the CDF and the average of the discovery times for different values of angular speed of the transceivers when $\beta = 25^\circ$. We observe that, for a fixed divergence angle, increasing the rotational/angular speed ω of the transceiver reduces the neighbor discovery time. From (8) and (9), we see that the average discovery time $t_{avg} \propto 1/\omega$, which is exactly what we observe in Fig. 8. For example, when

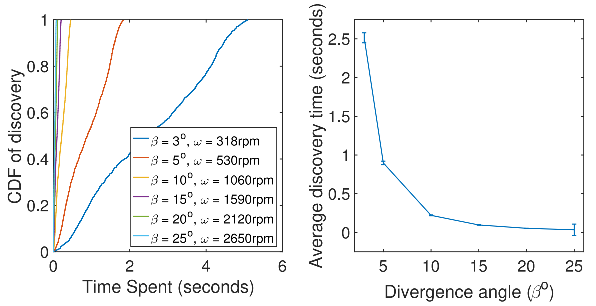

Fig. 9. CDF and average discovery time (95 percent confidence interval) for $\omega = \beta/\sqrt{2}\tau$.

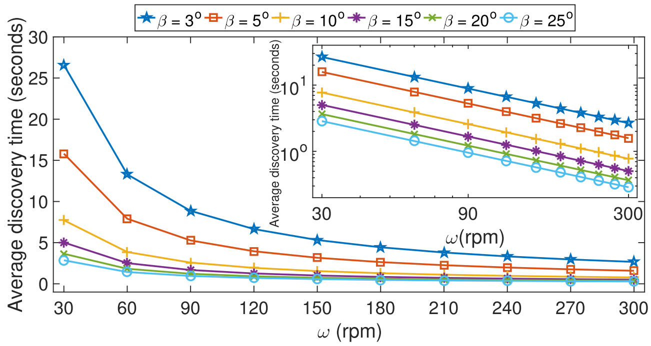

Fig. 10. Discovery Time versus ω for different β.

$\omega = 60$ rpm, neighbor discovery time can be as high as $3.2s$, but, when $\omega = 300$ rpm, neighbor discovery is completed within $0.64s$.

Fig. 9 shows the results where ω is calculated using (5), i.e., it is set to the sufficient value of angular speed. Similar to the previous results, we observe that higher values of divergence angles yield smaller discovery times. The average discovery time decreases as β and ω increases. Again, we see that $t_{avg} \propto 1/\omega \propto 1/\beta$. Moreover, we observe that, if the angular speed is very high, for example, $\approx 2,650$ rpm when $\beta = 25^\circ$, then the neighbor discovery can be completed within 0.07 s.

In Fig. 10, the combined effect of ω and β on average discovery time is presented. We can observe that, the discovery time reduces as divergence angle is increased. And also, increasing the angular speed also reduces discovery time, thus, improves the performance. Thus, larger divergence angle combined with faster rotational speed provides better performance than smaller divergence angle combined with slower rotational speed. For example, when $\beta = 3^\circ$ and $\omega = 30$ rpm, average discovery time is 26.592, but when $\beta = 25^\circ$ and $\omega = 300$ rpm, average discovery time is only $0.28s$. The figure in the inner box shows the result with both x-axis and y-axis in logarithmic scale. This result shows that, the differences between average discovery times for different divergence angles remains very consistent as rotational speed is varied.

Another aspect to look at is how much additional benefit is possible as ω becomes greater than the level sufficient to guarantee discovery when the transceivers face each other, i.e., $\omega_s = \beta/\sqrt{2}\tau$. Fig. 11 portrays the effect on average discovery time with 95 percent confidence when ω varies with respect to ω_s, where $\omega_s = \beta/\sqrt{2}\tau$. In Section 3.4.1, it was mentioned that when the beams of two transceivers start facing each other, the master node may not immediately start sending a Beacon. So, the required rotational speed

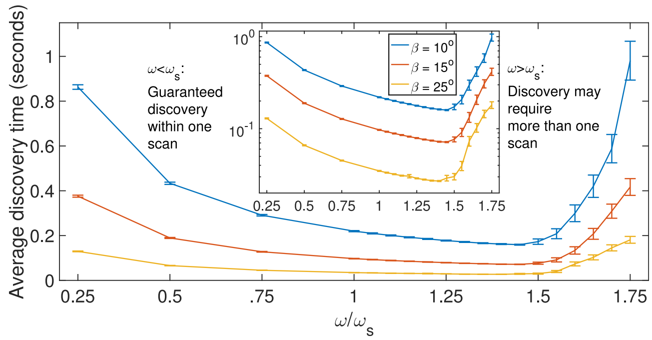

Fig. 11. Effect on discovery time as ω is varied with respect to $\omega_s = \beta/\sqrt{2}\tau$.

TABLE 2
Parameters for Simulating Hovering Errors

Setting	Horizontal error in m	Vertical error in m
HE^0	0	0
HE^1	(0.0, 0.5]	(0.0, 0.5]
HE^2	(0.5, 1.5]	(0.5, 1.5]
HE^3	(1.5, 3.0]	(0.5, 3.0]

was set to $\omega \leq \beta/\sqrt{2}\tau$ to ensure the completion of the three-way handshake and thus achieve neighbor discovery within one complete scan. The results in Fig. 11 demonstrate that when $\omega > \beta/\sqrt{2}\tau$, the nodes may not always complete the three-way handshake while their beams cross over each other. And hence, the nodes require multiple scans of the surrounding 3D space, which results in increased neighbor discovery time. Similar to the results displayed in Figs. 8 and 9, we can observe that the average discovery time keeps decreasing as ω increases. But we can see that, for $\omega \geq 1.5 \times \omega_s$, the average discovery time increases with increase in ω. This result shows an interesting phenomenon that the ideal setting for ω is around $1.5 \times \omega_s$.

4.2 Effect of Hovering Position Error

As mentioned earlier, we considered DJI Matrice 100 ($M100$) [36] drones as nodes. The $M100$ has hovering error of 2.5m horizontally and 0.5m vertically. So, we added the error values given in Table 2 to the drones' hovering positions in the simulations to observe how they affect the performance of the proposed neighbor discovery algorithm. Due to the hovering error, it is now possible that our 3D scans may not result in a complete neighbor discovery. So, in this section, we consider, the percentage of the number of times (out of 2000 simulation runs) discovery is completed within one complete scan ($P_{success}$) of the surrounding 3D network, as the performance metric.

Fig. 12 displays how the neighbor discovery times are affected by hovering error for different values of rotational speed, ω. The values of β and R_{max} were fixed at 3 Degree and 25m respectively. We can see that, for all values of ω, $P_{success}$ decreases as error is increased from HE^1 to HE^3. Moreover, we can observe that $P_{success}$ decreases as ω increases. Earlier, in Fig. 8, we observed that the performance of the neighbor discovery method was better for faster rotational speeds, considering average discovery time as the performance metric. Now, we can see that, in the presence of hovering error, considering $P_{success}$ as the performance metric, the neighbor discovery algorithm performs better for slower rotational speeds.

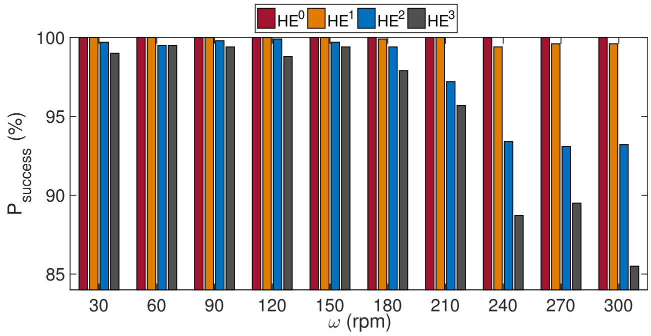

Fig. 12. Effect of hovering error for different values of ω.

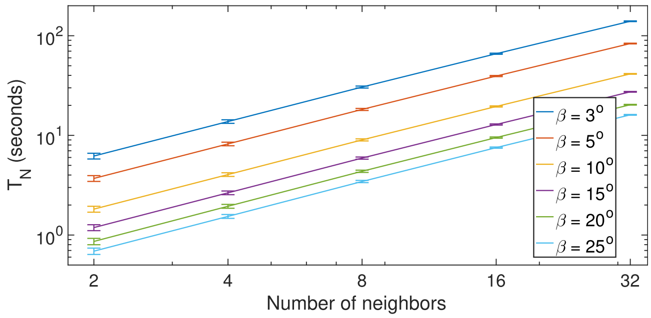

Fig. 13. Time taken to discover multiple neighbors using I-MND (both axes in logarithmic scale), 95 percent confidence interval.

We also performed simulations by varying the divergence angle for a fixed $\omega = 300$ rpm and $R_{max} = 50$m. We observed that, for $\beta = 3^0$ and $\beta = 5^\circ$, neighbor discovery is not completed 100 percent of the time within one complete scan as hovering error increases. For example, when $\beta = 3^\circ$ and error value is HE^2, discovery is successful within one scan $P_{success} = 87\%$ of the time; and, when $\beta = 3^\circ$ and error value is HE^3, $P_{success} = 84\%$. For larger divergence angles, such as, $\beta \geq 10^\circ$, $P_{success} = 100\%$, even in the presence of hovering error. Next, we varied R_{max} in our simulations and observed that $P_{success}$ improves as R_{max} increases. So, we can say that, as the coverage volume of the transceivers increases with increase in divergence angle or R_{max}, the hovering error has lesser effect on the neighbor discovery process.

4.3 Multiple Neighbors

In this section, we demonstrate how the proposed neighbor discovery scheme performs in multiple neighbor scenarios. We conducted simulations using the two approaches I-MND and L-MND described in Section 3.6. In both cases, we considered $R_{max} = 100m$ and $\omega = 300$rpm. Fig. 13 portrays the time required, T_N, for all neighbors in a network to discover each other using I-MND for different values of divergence angle β. We can observe that T_N increases linearly with the increase in number of nodes in the network. We can also see that, similarly to the single neighbor scenario, the discovery time decreases as β becomes larger.

Fig. 14 demonstrates the time taken to discover all neighbors for each node using L-MND. We assume that collision occurs when two or more nodes try to send packets to the same receiving node at the same time and the receiving node's transceiver's FOV is including both the sender nodes' beacons. We can again see that T_N increases as the number of nodes in the network increases. Also, we can observe that, when the number of nodes in the network is 3, 5 or 9 (number of neighbors: 2, 4, 8 respectively), T_N is smaller for larger values of divergence angle. But, when there are 16 neighbors or 17 nodes, $T_N = 4.68s$ for $\beta = 20^\circ$ and $T_N = 4.76s$ for $\beta = 25^\circ$. This phenomenon is the result of collision between packets. A transceiver beam with $\beta = 25^\circ$ covers more volume than a beam with $\beta = 20^\circ$, thus, the probality of it being in LOS with more nodes increases. Hence, the probabilty of collision increases with increase in β when there is a large number of nodes in a network. We can see that, for a network with 33 nodes, the effect of collision on neighbor discovery time is more prominent. Here, $T_N = 10.59$ s for $\beta = 20^\circ$ is higher than $T_N = 10.13$ for $\beta = 15^\circ$. Also, $T_N = 14.62$ s for $\beta = 25^\circ$ is higher than the values of T_N for both $\beta = 15^\circ$ and 20°. Fig. 15 portrays the effect of collision more clearly. We can see that collision does not affect neighbor discovery time when β is 3 or 5 Degree. But, for larger values of β (e.g., 10-25 Degree), neighbor discovery time increases as a result of collision.

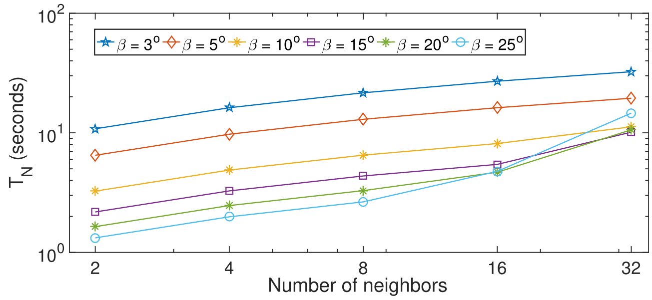

Fig. 14. Time taken to discover multiple neighbors using L-MND (both axes in logarithmic scale).

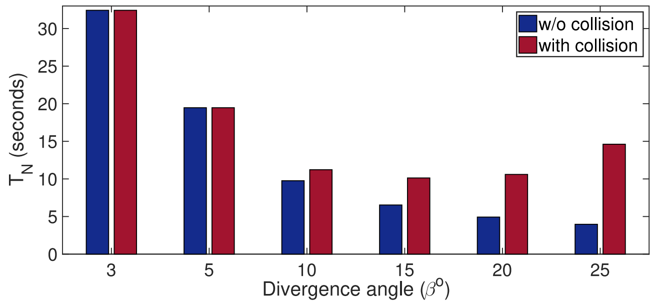

Fig. 15. Effect of packet collision on neighbor discovery time.

In Fig. 16, the neighbor discovery times achieved using I-MND and L-MND are compared. We can see that, for all different values of β, neighbor discovery tims ares smaller for I-MND than those for L-MND, when the number of nodes (M) in the network is small ($M \leq 5$). For higher number of nodes in the network, L-MND provides smaller discovery times compared to I-MND. We can observe that, because of the collision effect, the T_N achieved using L-MND is very close to the T_N acquired using I-MND for $\beta = 25^\circ$.

4.4 Summary of Simulation Results

- LOS discovery is guaranteed within one complete scan of the surrounding 3D space as long as $\omega \leq \frac{\beta}{\sqrt{2}\tau}$.
- Multiple scans may be required for discovery if $\omega > \frac{\beta}{\sqrt{2}\tau}$. For $\omega \geq 1.5\frac{\beta}{\sqrt{2}\tau}$, discovery time increases with ω.
- Wider transceiver beamwidth results in significant improvement in LOS discovery performance. Although, in case of multiple neighbor discovery wider beamwidth may increase the probability of collision.

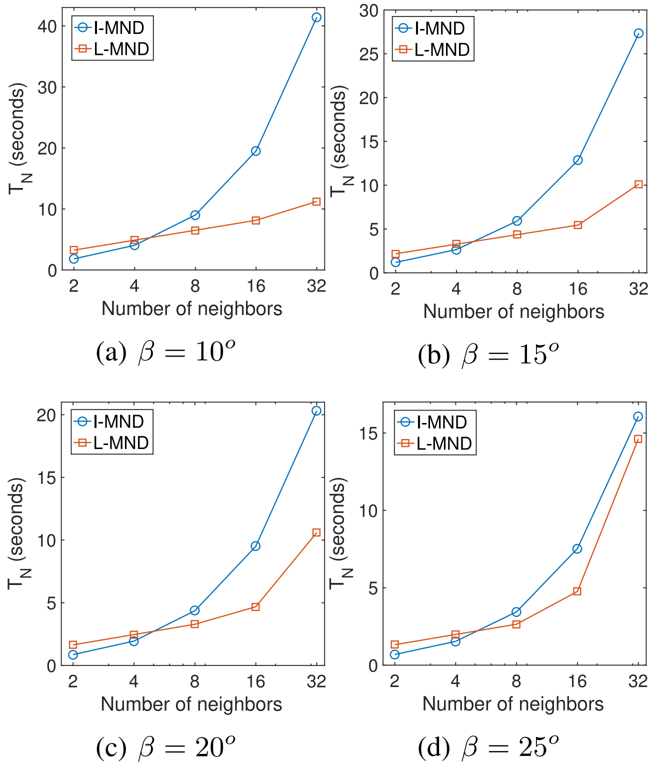

(a) $\beta = 10^o$ (b) $\beta = 15^o$

(c) $\beta = 20^o$ (d) $\beta = 25^o$

Fig. 16. I-MND versus L-MND (x-axis in logarithmic scale) when $\omega = 300\ rpm$.

- Faster rotation of the mechanically steerble head helps achive faster neighbor discovery.
- In the presence of error in the hovering position of the drones, probability of discovery within a single scan decreases. For divergence angle $\beta \geq 10^\circ$, the effect of hovering position error is negligible.
- In the multiple neighbor scenario, I-MND performs better for small networks ($\leq$5 nodes) and L-MND provides faster discovery times for larger (>5 nodes) network size.
- For L-MND, discovery times may increase because of packet collisions. As the number of nodes in the network increases, the collision effect becomes more prominent. For small divergence angles like 3 or 5 Degree, the effect of packet collision is negligible.

4.5 Comparison With State-of-the-Art Methods

The neighbor discovery protocols presented by Zhang et al. [3], [29] are designed for LOS discovery in 2D and then extended to 3D. The authors considered a scan based algorithm (SBA-D), where a sphere can ideally be divided into some sectors according to the framework given in [30]. Zhang [3], [29] provides significant proof and details for beam scanning mechanism in 2D. But, it does not provide the detailed beam scanning method for 3D ad hoc networks. To get the number of scans theoretically, it relies on the formula $\frac{2}{1-\cos\beta}$, which actually is the lower bound on the number of cones that can cover a sphere given by Steenstrup [30]. However, the study does not provide any specific scan sequence that the transceivers can follow to scan the surrounding 3D space. In this paper, we fill this gap by providing a concrete scan sequence and the path along which a transceiver should rotate to cover the entire surface of a sphere.

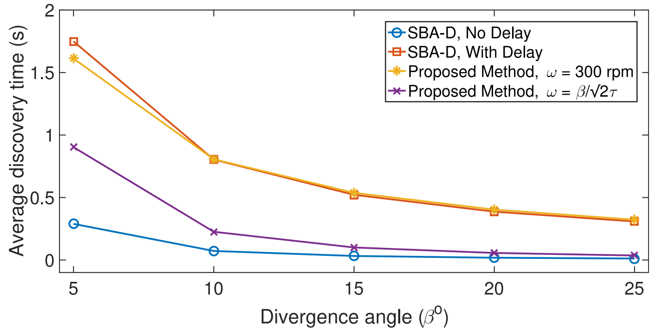

Fig. 17. Comparison of average discovery time in the proposed mechanism to SBA-D [3].

From the mathematical model of SBA-D in [3], we analyzed the average time for neighbor discovery. Note that, here we use the same equation as used by the paper and simply assume that the neighbors are discovered within a single full scan of the sphere, although in practice, if a direction is not covered in any cone, neighbor in that direction would not be discovered. We analyzed two methods: In the first one, we consider instantaneous beam switching, i.e., there is no delay in switching the beam from one sector to another. In the second, we present another set of results considering switching delay. Here, switching delay is $2\beta/\omega$ where β is the divergence angle and ω is the angular speed (in this case, we consider $\omega = 300$ rpm). Basically, it roughly determines the time to go from one cone to an adjacent cone. Note that this is not very realistic because, in mechanical steering, the transceivers need some time to accelerate and some time to stop rotating. We present the reults in Fig. 17 and compare it with the results of our proposed mechanism. To compare our results, we present the average discovery time considering the sufficient angular speed of our method ($\omega = \beta/\sqrt{2}\tau$) and a fixed value of $\omega = 300$ rpm. We can clearly see that our proposed method results in larger discovery times. However, as we stated earlier, these two mechanisms cannot be fairly compared because mechanical rotation constraints and a required scan sequence of beam directions need to be integrated to SBA-D.

5 Proof-of-Concept Prototype

We developed a proof-of-concept prototype to perform experimental evaluation of the proposed neighbor discovery method in a 3D environment. We used off-the-shelf electronic components to design and built the prototype. Fig. 20 shows the different parts of the prototype, which are: A DJI drone, a mechanically steerable head, and an IR transceiver. These parts are controlled by a Raspberry Pi [38] using separate threads: Head control, data transmission, and data reception. Fig. 18 shows the block diagram of the prototype system architecture.

5.1 System Hardware

5.1.1 DJI Drone

We used Matrice 100 drones/quadcopters (Fig. 20) as the nodes in our work. The Matrice 100 (M100) is a customizable quadcopter produced by DJI. It is a very stable and powerful flying platform. DJI has made it an open platform and is very suitable for researchers and developers. It has a hovering accuracy of 0.5m vertically and 2.5m horizontally, and can fly at a maximum speed of 22m/s. It can be controlled using a remote controller and can also be customized for autonomous operation using the DJI SDK [36].

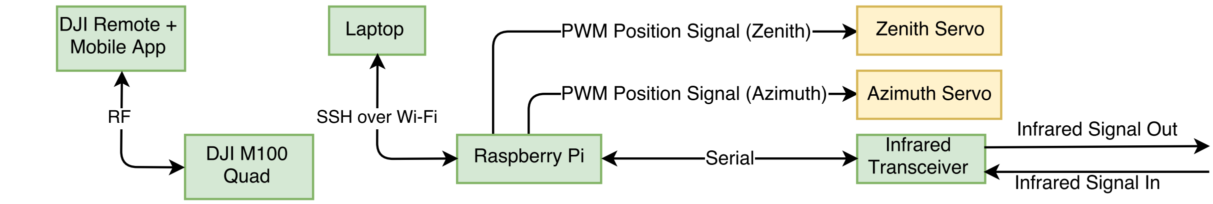

Fig. 18. Prototype block diagram.

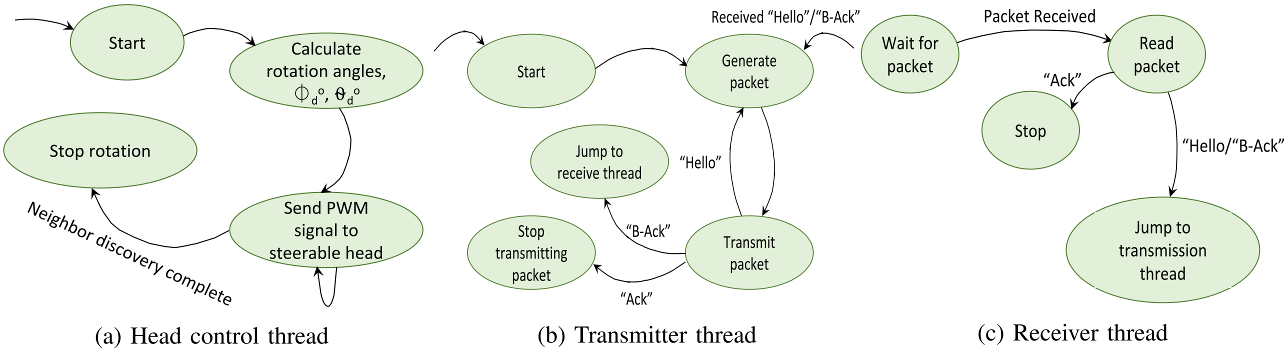

Fig. 19. Different threads running in the prototype.

5.1.2 Mechanically Steerable Head

We used a 2 DOF Pan and Tilt sensor mount [39] as the steerable head (Fig. 20) on which we mount the IR transceiver. The sensor mount consists of two Mg995 [40] servo motors controlled by a Raspberry PI. One servo provides rotation along the horizontal plane and the other one along the vertical plane. The combination of these rotations of the two servos help achieve 3D rotation.

5.1.3 The Transceiver

We used IrDA2 Click [41] as the transceiver. The board includes an infrared encoder/decoder. This device sits between a UART and an infrared (IR) optical transceiver. It supports IrDA speeds up to 115.2 Kbit/s. The transceiver module also has a photo pin diode, an infrared emitter (IRED), and a low-power control IC to provide a total front-end solution in a single package. The IrDA2 Click covers a maximum communication range of 3 meters using the internal intensity control. The infrared emitter has peak emission wavelength of 900 nm and divergence angle (angle of half intensity) of $\pm 24°$.

5.2 Implementing the Neighbor Discovery Protocol

We implemented the initialization phase (described in Section 3.3) using a simple client-server program in Python. The client program runs on the Master node and the server program runs on the Slave node. The PIs on the quadcopters/nodes are controlled from a laptop via a secure shell session (SSH) over Wi-Fi (2.4 GHz ISM band). The laptop and the PIs are all on the same local-area-network (LAN). The nodes are identified using their IP addresses in the LAN. The Master node sends message to a specific port of the other node. The Slave node keeps listening on that port. A simple three-way handshake through Wi-Fi helps synchronize the two nodes' mechanical head rotation before the start of the 3D scanning stage. Wi-Fi is not further used in the protocol. Since the Master node is always hovering at a higher elevation than the Slave node (it is either on the ground or hovering a lower elevation), we started the Master node's head rotation by facing downward ($\theta = 180°, \phi = 0°$) and the Slave node's head rotation facing upward ($\theta = 0°, \phi = 0°$) to minimize the discovery time.

In the 3D scanning stage, the nodes use three separate threads (running in the Raspberry PIs), one for running the servos (Fig. 19a), one for packet transmission (Fig. 19b) and the other for packet reception (Fig. 19c). The Master node starts rotating its head following the spiral pattern described in Sections 3.4 and 3.4.2. At the same time, it sends a 'Beacon' message every 5 ms using the IrDA2 Click and waits for a 'B-ACK'. The Slave node also starts scanning the 3D space following the spiral pattern and keeps listening for the 'Beacon' on its IR transceiver. When it receives a 'Beacon', it starts sending a 'B-ACK' every 5 ms and waits for an 'ACK'. The Master node receives this 'B-ACK' and stops rotating its head. It sends an 'ACK' and stops all its threads. The Slave then stops all its threads when it receives an 'ACK'. And, this marks the end of the 3D neighbor discovery.

5.3 System Limitations

The servo motors used to rotate the heads could only perform a maximum of 180 Degree rotation. So, we emulated

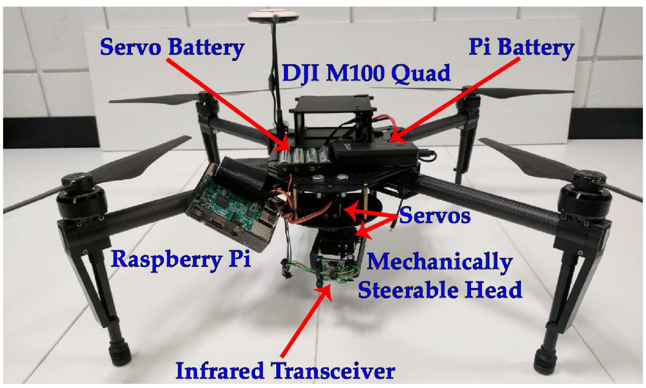

Fig. 20. Front view of the proof-of-concept prototype.

(a) Sanity check: One node hovering on top of the other

(b) Sanity check: Both nodes hovering at the same height

(c) Find discovery time: One on ground, another hovering

(d) Find discovery time: Both nodes hovering

Fig. 21. Snapshots of experiments coducted using the develpoed proof-of-concept prototype.

the 181 to 360 Degree rotation along the horizontal plane (x-y plane), by performing rotation in the opposite direction, from 179 to 0 Degree, once it reached 180 Degree. We made sure that the nodes do not transmit or receive packets during the 179-0 Degree horizontal steering. The maximum angular speed of the steering head was 180 Degree/s. Also, we mounted the steerable head on top of one of the drones. During the experiments, we kept this drone on the ground. For the other drone, the head was placed at the bottom. We made this drone hover at a higher elevation than the other one for all experimental scenarios. Other limitations are: the communication range of the transceivers is 3 meters and the data transfer rate of the transceivers is 115.2 Kbps.

5.4 Experimental Results

We performed experimental evaluation of our proposed directional neighbor discovery protocol using the developed prototype. First, we kept one node on the ground and the other one hovering. The ground node was the Master and the hovering node was the Slave. Next, we performed further experiments by hovering both nodes above the ground. The Master node always started the 3D scanning by facing upward ($\phi = 0^\circ, \theta = 0^\circ$) and the Slave node faced downward ($\phi = 0^\circ, \theta = 180^\circ$). We performed two experiments, one for checking the sanity of the proposed algorithm and another for measuring the neighbor discovery time.[1]

5.4.1 Sanity Check

The goal of this experiment is to show the sanity of the proposed LOS discovery protocol. In this experiment, Master node was on the ground and Slave node was hovering. As shown in Fig. 21a, the Slave node was kept in a hovering position right on top of the Master node, and ω was fixed at 180 Degree/s. In one scenario, the Master started the 3D scan facing its transceiver upward ($\phi = 0^\circ, \theta = 0^\circ$), and the Slave started the scan facing its transceiver downward ($\phi = 0^\circ, \theta = 180^\circ$). We ran the experiment 10 times, and, the nodes almost immediately (≈ 0.55 s-0.65 s) discovered each other, since they started the scan facing their transceivers directly at each other. In another scenario, the Master started the 3D scan facing its transceiver downward ($\phi = 0^\circ, \theta = 180^\circ$), and the Slave started the scan facing its transceiver upward ($\phi = 0^\circ, \theta = 0^\circ$). So, the transceivers were facing away from each other. We again ran the experiment 10 times, and, in this case, both nodes had to perform a complete 3D scan before discovering each other. The discovery time was ≈ 6.2 s-6.8 s in this scenario. We performed further experiments by hovering both drones at approximately the same altitute from the ground (Fig. 21b). We collected 10 data points by changing the horizontal position of the Slave. In this case, the discovery times were between 4.63 s and 4.89 s.

5.4.2 Discovery Time

The aim of this experiment was to find out the neighbor discovery time in the 3D scanning stage. First, Master node was kept on the ground and Slave node hovered within the communication radius of 3 meters as shown in Fig. 21c. We performed the experiment for four different values of rotational speed of the mechanical head. We acquired 99 data points for $\omega = 90^\circ$/s, 112 for $\omega = 120^\circ$/s, 116 for $\omega = 150^\circ$/s, and 91 for $\omega = 180^\circ$/s. Fig. 22 shows the cumulative distribution function (CDF) and average of the discovery times achieved from the experiments. We can observe that, the discovery time reduces as ω increases. This means that, higher rotational speed helps a node discover a neighbor faster than lower rotational speed. This result is consistent with the simulation results presented in Section 4.1. Next, we repeated the experiments by hovering

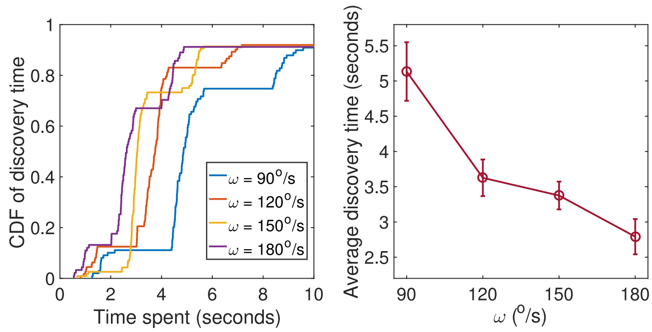

Fig. 22. CDF and average discovery time (95 percent confidence interval) for one node on ground and one hovering node.

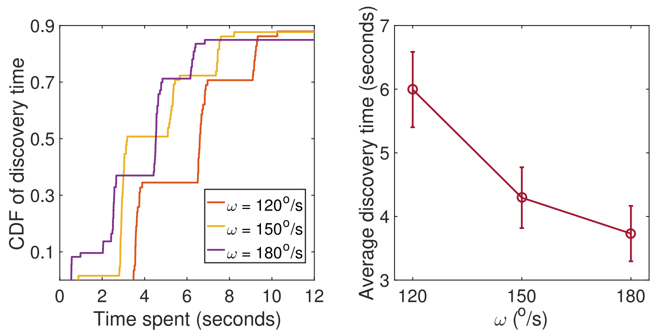

Fig. 23. CDF and average discovery time (95 percent confidence interval) for both nodes hovering above ground.

1. A video displaying some sample experiments is provided here: https://youtu.be/1upQaw86ZsE

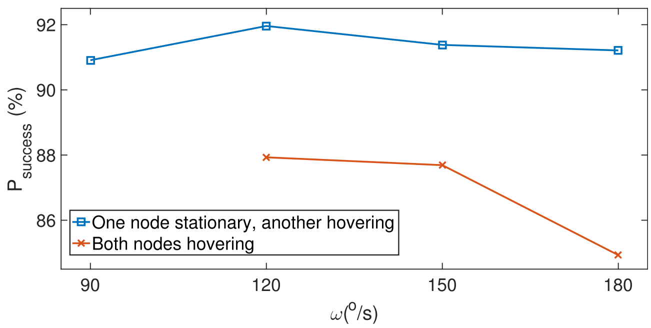

Fig. 24. Probability of discovery within one full scan is less than 100 percent because of hovering position error.

both nodes above ground (Fig. 21d) for three separate angular speeds and gathered 58 data points for $\omega = 120^\circ/\text{s}$, 65 for $\omega = 150^\circ/\text{s}$ and 74 for $\omega = 180^\circ/\text{s}$. The results are displayed in Fig. 23, where we can observe that the average discovery times are higher than the case when only one node was hovering. This is caused by the cases when the Master node hovers at a higher altitude than the Slave node and since the Master always started the 3D scanning by facing upward ($\phi = 0^\circ, \theta = 0^\circ$) and the Slave faced downward ($\phi = 0^\circ, \theta = 180^\circ$) at the start.

During the experiments, we observed that, due to error in the hovering position, the nodes could not complete the discovery within one complete scan of the surrounding environment in some cases. This result is displayed in Fig. 24. Here, P_{succes} represents the percentage of the time the two nodes discovered each other within one scan. We can observe that, when one node is hovering, for all values of ω, discovery was complete within one scan more than 90 percent of the time. We also observe that, as ω increases from 120 to 180 Degree/s, $P_{success}$ reduces, similar to our observations in the simulation results presented in Section 4.2. But, we can also see here, for $\omega = 90^\circ/\text{s}$, $P_{success}$ is lower than those achieved with other values of ω. The results demonstrates that, even when both nodes were in hovering positions, discovery was complete within one scan more than 85 percent of the time in all cases.

6 Conclusion

We proposed a novel scheme for neighbor discovery in a 3D ad-hoc network. The scheme is a hybrid design in that it makes an initial synchronization of the nodes via an additional channel and then resorts to asynchronous 3D scanning to complete the discovery process. We consider nodes (UAVs or quadcopters) hovering in 3D space, each equipped with a mechanically steerable head/arm on which a highly directional FSO or RF transceiver is mounted. The nodes rotate their transceivers following a modified spiral path and send/receive search signals to discover each other. We showed that, for very fast rotational speeds of the transceivers, neighbor discovery can be performed even within 0.034s. We observed that the neighbor discovery algorithm provides better performance with faster rotational speed and larger divergence angle of transceivers. But, in the presence of hovering position of the nodes, miss detection increases with increased rotational speed. We proposed two schemes for neighbor discovery when there are multiple neighbors present in the network. Through extensive simulations we demonstrated that all the nodes in the network can discover all of their neighbors successfully. From the simulation results we observed that I-MND performs better for small networks and L-MND provides better performance for larger networks. Additionally, we designed and built a proof-of-concept prototype using off-the-shelf components. We conducted experiments using the developed prototype to demonstrate the effectiveness of the proposed method. The results from both simulations and experiments show that, using the proposed neighbor discovery algorithm, the nodes in a 3D wireless network can successfully discover each other within a very small amount of time. The current prototype implementation is limited by the IrDA2's communication speed of 115.2 Kbps and range of 3 meters.

We want to improve the prototype by using transceivers of different divergence angles, faster communication speed and larger range. We also plan to perform experiments using multiple drones. A key design decision in our work is the use of an additional RF channel for initial synchronization. We plan to develope a neighbor discovery algorithm that would not depend on any additional RF channel other than only one highly directional transceiver for each node in a 3D wireless ad-hoc network.

Acknowledgments

This work was supported in part by NSF award 1663764. An earlier version of this work appeared in IEEE MILCOM 2016 [1].

References

[1] M. Khan, S. Bhunia, M. Yuksel, and S. Sengupta, “LOS discovery in 3D for highly directional transceivers,” in *Proc. IEEE Military Commun. Conf.*, 2016, pp. 325–330.

[2] R. R. Choudhury, X. Yang, R. Ramanathan, and N. H. Vaidya, “Using directional antennas for medium access control in ad hoc networks,” in *Proc. 8th Annu. Int. Conf. Mobile Comput. Netw.*, 2002, pp. 59–70.

[3] Z. Zhang and B. Li, “Neighbor discovery in mobile ad hoc self-configuring networks with directional antennas: Algorithms and comparisons,” *IEEE Trans. Wireless Commun.*, vol. 7, no. 5, pp. 1540–1549, May 2008.

[4] G. Pei, M. M. Albuquerque, J. H. Kim, D. P. Nast, and P. R. Norris, “A neighbor discovery protocol for directional antenna networks,” in *Proc. IEEE Military Commun. Conf.*, 2005, pp. 487–492.

[5] M. Khan, M. Yuksel, and G. Winkelmaier, “GPS-free maintenance of a free-space-optical link between two autonomous mobiles,” *IEEE Tran. Mobile Comput.*, vol. 16, no. 6, pp. 1644–1657, Jun. 2017.

[6] A. Mpitziopoulos, D. Gavalas, C. Konstantopoulos, and G. Pantziou, “A survey on jamming attacks and countermeasures in wsns,” *IEEE Commun. Surveys Tuts.*, vol. 11, no. 4, Oct.-Dec. 2009.

[7] S. Bhunia, V. Behzadan, P. A. Regis, and S. Sengupta, “Performance of adaptive beam nulling in multihop ad-hoc networks under jamming,” in *Proc. IEEE 17th Int. Conf. High Perform. Comput. Commun/IEEE 7th Int. Symp. Cyberspace Safety Secur/IEEE 12th Int. Conf. Embedded Softw. Syst.*, 2015, pp. 1236–1241.

[8] S. Bhunia, V. Behzadan, P. A. Regis, and S. Sengupta, “Adaptive veam nulling in multihop ad hoc networks against a jammer in motion,” *Comput. Netw.*, vol. 109, pp. 50–66, 2016.

[9] S. Bhunia, P. A. Regis, and S. Sengupta, “Distributed adaptive beam nulling to survive against jamming in 3d uav mesh networks,” *Comput. Netw.*, vol. 137, pp. 83–97, 2018.

[10] D. Weatherington and U. Deputy, “Unmanned aircraft systems roadmap, 2005–2030,” *Deputy, UAV Planning Task Force, OUSD*, Office of the Secretary of Defense, 2005, https://fas.org/irp/program/collect/uav_roadmap2005.pdf

[11] E. Leitgeb, K. Zettl, S. Muhammad, N. Schmitt, and W. Rehm, “Investigation in free space optical communication links between UAVs,” in *Proc. 9th Int. Conf. Transparent Opt. Netw.*, 2007, pp. 152–155.

[12] R. Sun and D. W. Matolak, “Over-harbor channel modeling with directional ground station antennas for the air-ground channel,” in *Proc. IEEE Military Commun. Conf.*, 2014, pp. 382–387.

[13] J. Chen, J. Xie, Y. Gu, S. Li, S. Fu, Y. Wan, and K. Lu, “Long-range and broadband aerial communication using directional antennas (acda): Design and implementation,” *IEEE Trans. Veh. Technol.*, vol. 66, no. 12, pp. 10793–10805, Dec. 2017.

[14] Facebook Laser Communication. [Online]. Available: https://www.facebook.com/zuck/videos/10102274951725301/

[15] Facebook demonstrates record-breaking data rate using millimeter-wave technology, 2016. [Online]. Available: https://code.facebook.com/posts/1197678800270377/facebook-demonstrates-record-breaking-data-rate-using-millimeter-wave-technology/

[16] R. R. Choudhury, X. Yang, R. Ramanathan, and N. H. Vaidya, “On designing MAC protocols for wireless networks using directional antennas,” *IEEE Trans. Mobile Comput.*, vol. 5, no. 5, pp. 477–491, May 2006.

[17] S. Yi, Y. Pei, and S. Kalyanaraman, “On the capacity improvement of ad hoc wireless networks using directional antennas,” in *Proc. 4th ACM Int. Symp. Mobile Ad Hoc Netw. Comput.*, 2003, pp. 108–116s.

[18] R. Ramanathan, J. Redi, C. Santivanez, D. Wiggins, and S. Polit, “Ad hoc networking with directional antennas: A complete system solution,” *IEEE J. Select. Areas Commun.*, vol. 23, no. 3, pp. 496–506, Mar. 2005.

[19] G. Noubir, “On connectivity in ad hoc networks under jamming using directional antennas and mobility,” in *Proc. Int. Conf. Wired/Wireless Internet Commun.*, 2004, pp. 186–200.

[20] S. Bhunia and S. Sengupta, “Distributed adaptive beam nulling to mitigate jamming in 3D UAV mesh networks,” in *Proc. Int. Conf. Comput. Netw. Commun.*, 2017, pp. 120–125.

[21] M. Khan and M. Yuksel, “Autonomous alignment of free-space-optical links between UAVs,” in *Proc. 2nd Int. Workshop Hot Top. Wireless*, 2015, pp. 36–40.

[22] X. An and R. Hekmat, “Self-adaptive neighbor discovery in ad hoc networks with directional antennas,” in *Proc. 16th IST Mobile Wireless Commun. Summit*, 2007, pp. 1–5.

[23] S. Vasudevan, J. Kurose, and D. Towsley, “On neighbor discovery in wireless networks with directional antennas,” in *Proc. 21st Signal Process. Commun. Appl. Conf.*, 2005, pp. 1–4.

[24] G. Jakllari, W. Luo, and S. V. Krishnamurthy, “An integrated neighbor discovery and mac protocol for ad hoc networks using directional antennas,” *IEEE Trans. Wireless Commun.*, vol. 6, no. 3, pp. 1114–1024, Mar. 2007.

[25] L. Chen, Y. Li, and A. V. Vasilakos, “On Oblivious Neighbor Discovery in Distributed Wireless Networks With Directional Antennas: Theoretical Foundation and Algorithm Design,” *IEEE/ACM Trans. Netw.*, vol. 25, no. 4. pp. 1982–1993, Aug. 2017.

[26] Y. Wang, S. Mao, and T. S. Rappaport, “On Directional Neighbor Discovery in mmWave Networks,” in *Proc. IEEE 37th Int. Conf. Distrib. Comput. Syst.*, 2017, pp. 1704–1713.

[27] S. Bhunia, M. Khan, S. Sengupta, and M. Yuksel, “LOS discovery for highly directional full duplex RF/FSO transceivers,” in *Proc. IEEE Military Commun. Conf.*, 2016, pp. 337–342.

[28] M. Khan and M. Yuksel, “In-band los discovery between drones using highly directional transceivers,” in *Proc. 4th ACM Workshop Micro Aerial Vehicle Netw. Syst. Appl.*, 2018, pp. 51–56.

[29] Z. Zhang, “Performance of neighbor discovery algorithms in mobile ad hoc self-configuring networks with directional antennas,” in *Proc. IEEE Military Commun. Conf.*, 2005, pp. 3162–3168.

[30] M. E. Steenstrup, “Neighbor discovery among mobile nodes equipped with smart antennas,” in *Proc. Scandinavian Workshop Wireless Adhoc Netw.*, 2003, pp. 1–6.

[31] K. Nakano and S. Olariu, “A survey on leader election protocols for radio networks,” in *Proc. Int. Symp. Parallel Archit. Algorithms Netw.*, 2002, pp. 71–76.

[32] J. Villadangos, A. Cordoba, F. Fariña, and M. Prieto, “Efficient leader election in complete networks,” in *Proc. 13th Euromicro Conf. Parallel Distrib. Netw.-Based Process.*, 2005, pp. 136–143.

[33] N. Santoro, *Design and Analysis of Distributed Algorithms*, vol. 56. Hoboken, NJ, USA: Wiley, 2006.

[34] E. Chang and R. Roberts, “An improved algorithm for decentralized extrema-finding in circular configurations of processes,” *Commun. ACM*, vol. 22, no. 5, pp. 281–283, 1979.

[35] H. Attiya and J. Welch, *Distributed Computing: Fundamentals, Simulations, and Advanced Topics*, vol. 19. Hoboken, NJ, USA: Wiley, 2004.

[36] Matrice100: Quadcopter for developers. [Online]. Available: http://www.dji.com/matrice100

[37] M. Yuksel, J. Akella, S. Kalyanaraman, and P. Dutta, “Free-space-optical mobile ad hoc networks: Auto-configurable building blocks,” *Wireless Netw.*, vol. 15, no. 3, pp. 295–312, 2009.

[38] Raspberry Pi. [Online]. Available: https://www.raspberrypi.org/

[39] 2 DOF Pan and Tilt. [Online]. Available: https://www.amazon.com/Mallofusa-Mg995-Servos-Sensor-Arduino/

[40] MG995 servo motors. [Online]. Available: http://www.towerpro.com.tw/product/mg995/

[41] IrDA2 click. [Online]. Available: http://www.mikroe.com/click/irda2/

Mahmudur Khan received the BSc degree in electrical and electronic engineering from the Bangladesh University of Engineering and Technology, in 2011, the MS degree in computer science and engineering from the University of Nevada Reno, in 2015, and the PhD degree in computer engineering from the University of Central Florida, in 2018, respectively. He is a postdoctoral researcher with the ECE Department, University of Alabama. His research interests include the area of free-space-optical communications, wireless ad hoc networks, and UAV communications. He is a member of the IEEE.

Suman Bhunia received the bachelor’s degree in electronics and communication engineering from the West Bengal University of Technology, in 2008, the master’s degree in distributed and mobile computing from Jadavpur University, India, in 2010, and the PhD degree in computer science from the University of Nevada, Reno, in 2017. He is a postdoctoral scholar with the Texas A&M Univerisity, College Station. His research interest includes security and vulnerabilities in wireless communications.

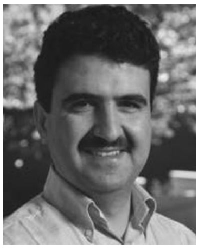

Murat Yuksel received the BS degree in computer engineering from Ege University, Izmir, Turkey, in 1996, and the MS and PhD degrees in computer science from RPI, in 1999 and 2002, respectively. He is an associate professor with the ECE Department, University of Central Florida (UCF), Orlando, Florida. Prior to UCF, he was with the CSE Department, University of Nevada, Reno (UNR), Reno, Nevada, as a faculty member until 2016. He worked as a software engineer with Pepperdata, Sunnyvale, California, and a visiting researcher with AT&T Labs and the Los Alamos National Lab. His research interests include networked, wireless, and computer systems with a recent focus on big-data networking, UAV networks, optical wireless, public safety communications, device-todevice protocols, economics of cyber-security and cybersharing, routing economics, network management, and network architectures. He has been on the editorial board of *Computer Networks*, and published more than 100 papers in peer-reviewed journals and conferences. He is a senior member of the IEEE, and a senior and life member of the ACM.

Lawrence C. Kane is working toward the BS degree in computer science at the University of Central Florida. Outside class, he volunteers to mentor less experienced students (especially fellow transfer students) in software engineering, helps host lectures for and manage the AI/data science club at UCF, and learns random tech for fun on the side (see github.com/ChasKane). He will pursue a master’s degree in data science after graduating from UCF in 2019.